

k_{\perp} Jet Algorithms in Hadron Colliders: The DØ Experience

V. Daniel Elvira*
Fermi National Accelerator Laboratory

DØ has implemented and studied a k_{\perp} jet algorithm for the first time in a hadron collider. We have submitted two physics results for publication: the subjet multiplicity in quark and gluon jets and the central inclusive jet cross section measurements. A third result, a measurement of thrust distributions in jet events, is underway. A combination of measurements using several types of algorithms and samples taken at different center-of-mass energies is desirable to understand and distinguish with higher accuracy between instrumentation and physics effects.

1. Introduction

Historically, only cone algorithms have been used to reconstruct jets at hadron colliders [1]. Although well-suited to the understanding of the experimental systematics present in the complex environment of hadron colliders, the cone algorithms used in previous measurements by the Fermilab Tevatron experiments [2, 3] present several difficulties: an arbitrary procedure must be implemented to split and merge overlapping calorimeter cones, an ad-hoc parameter, R_{sep} [4], is required to accommodate the differences between jet definitions at the parton and detector levels, and improved theoretical predictions calculated at the next-to-next-to-leading-order (NNLO) in pQCD are not infrared safe, but exhibit sensitivity to soft radiation [5].

A second class of jet algorithms, which does not suffer from these shortcomings, has been developed by several groups [6, 7, 8]. These recombination algorithms successively merge pairs of nearby objects (partons, particles, or calorimeter towers) in order of increasing relative transverse momentum. A single parameter, D , which approximately characterizes the size of the resulting jets, determines when this merging stops. No splitting or merging is involved because each object is uniquely assigned to a jet. There is no need to introduce any ad-hoc parameters, because the same algorithm is applied at the theoretical and experimental level. Furthermore, by design, clustering algorithms are infrared and collinear safe to all orders of calculation.

For the first time in a hadron collider, the DØ Collaboration has implemented a k_{\perp} algorithm to reconstruct jets from data taken during the 1992-1995 period (Run I). This paper is a summary of the DØ experience implementing and understanding the k_{\perp} algorithm, as well as a review of the associated measurements recently performed by the DØ experiment [9, 10].

2. The Run I DØ Detector

DØ is a multipurpose detector designed to study $p\bar{p}$ collisions at the Fermilab Tevatron Collider. A full description of the DØ detector can be found in Ref. [11]. The primary detector components for jet measurements at DØ are the calorimeters, which use liquid-argon as the active medium and uranium as the absorber. The DØ calorimetry provides full solid angle coverage and particle containment (except for neutrinos or high p_T muons), as well as linearity of response with energy and compensation (e/π response ratio is less than 1.05). Figure 1 shows a schematic view of one quadrant of the DØ calorimeter in the $r - z$ plane. Radial lines illustrate the detector pseudorapidity ($\eta = -\ln \tan \theta/2$), and the pseudo-projective geometry of the calorimeter towers. Each tower is composed of unit cells (rectangles in grey and white) with a size of $\Delta\eta \times \Delta\phi = 0.1 \times 0.1$. The single particle energy resolutions for electrons (e) and pions (π), measured from test beam data, are approximately 15% and 50% respectively.

*daniel@fnal.gov; <http://www-pat.fnal.gov/personal/daniel/>;

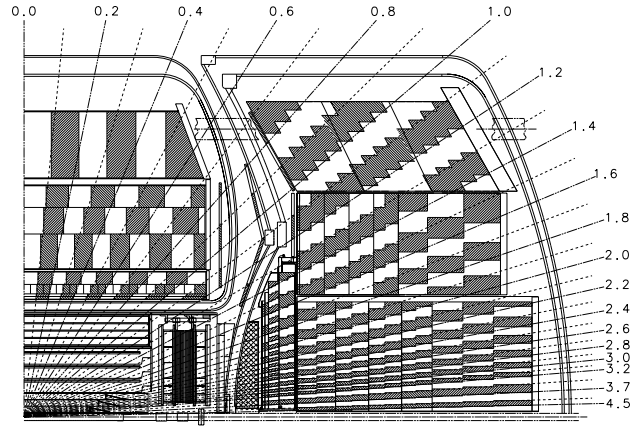


Figure 1: One quadrant of the DØ calorimeter and drift chambers, projected in the $r - z$ plane.

The energy of a particle measured in the calorimeters is distorted by energy deposits due to uranium decays, spectator partons, multiple $p\bar{p}$ interactions in the same beam crossing, and pile-up of electronic signals slowly decaying from previous crossings. Other factors affecting the energy measurement include non-uniformities from poorly instrumented regions, particle showering in the calorimeter, and resolution effects. (See Ref. [9].) Physics objects are reconstructed from energy depositions in calorimeter cells using algorithms. It is not possible to establish a one-to-one correspondence between a particle which struck the calorimeter and a calorimeter cell or tower. One particle is typically associated with many cells and vice-versa.

3. k_{\perp} jet algorithm

The DØ k_{\perp} jet algorithm [9] starts with a list of energy preclusters, formed from calorimeter cells or from particles in a Monte Carlo event generator. The preclusters are separated by $\Delta\mathcal{R} = \sqrt{\Delta\eta^2 + \Delta\phi^2} > 0.2$, where η and ϕ are the pseudorapidity and azimuthal angle of the preclusters. The steps of the jet algorithm are:

1. For each object i in the list, define $d_{ii} = p_{T,i}^2$, where p_T is the energy transverse to the beam.

For each pair (i, j) of objects, also define $d_{ij} = \min(p_{T,i}^2, p_{T,j}^2) \frac{\Delta\mathcal{R}_{ij}^2}{D^2}$, where D is a parameter of the jet algorithm.

2. If the minimum of all possible d_{ii} and d_{ij} is a d_{ij} , then replace objects i and j by their 4-vector sum and go to step 1. Else, the minimum is a d_{ii} so remove object i from the list and define it to be a jet.

3. If any objects are left in the list, go to step 1.

The algorithm produces a list of jets, each separated by $\Delta\mathcal{R} > D$.

Subjets may be defined by rerunning the k_{\perp} algorithm starting with a list of preclusters in a jet. Pairs of objects with the smallest d_{ij} are merged successively until all remaining $d_{ij} > \mathcal{Y}_{\text{cut}} p_T^2(\text{jet})$. The resolved objects are called subjets, and the number of subjets within the jet is the subjet multiplicity M . For $\mathcal{Y}_{\text{cut}} = 1$, the entire jet consists of a single subjet ($M = 1$). As \mathcal{Y}_{cut} decreases, the subjet multiplicity increases, until every precluster becomes resolved as a separate subjet in the limit $\mathcal{Y}_{\text{cut}} \rightarrow 0$.

4. Calibration of jet momentum

The uncertainty in the jet energy or momentum is the dominant systematic in almost every jet measurement at a hadron collider. The calibration at DØ accounts not only for detector effects, but also for the contribution of the underlying event (momentum transferred as a result of the soft interactions between the remnant partons of the proton and antiproton), and multiple $p\bar{p}$

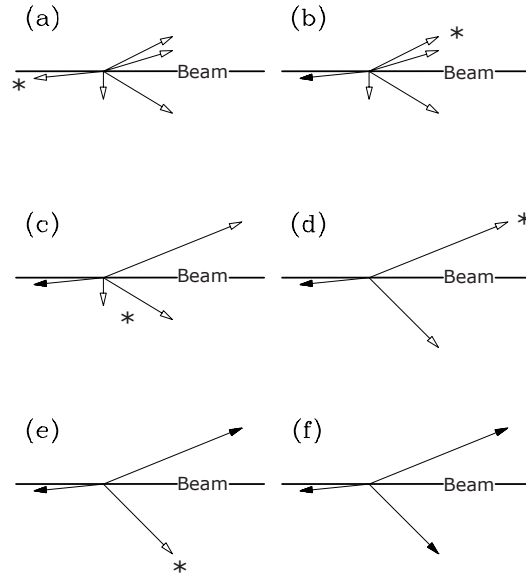


Figure 2: A simplified example of the final state of a collision between two hadrons. (a) The particles in the event (represented by arrows) comprise a list of objects. (b-f) Solid arrows represent the final jets reconstructed by the k_{\perp} algorithm, and open arrows represent objects not yet assigned to jets. The five diagrams show successive iterations of the algorithm. In each diagram, a jet is either defined (when it is well-separated from all other objects), or two objects are merged (when they have small relative k_{\perp}). The asterisk labels the relevant object(s) at each step.

interactions. All such corrections enter in the relation between the momentum of a jet measured in the calorimeter p^{meas} and the “true” jet momentum p^{true} [12]

$$p_{\text{jet}}^{\text{true}} = \frac{p_{\text{jet}}^{\text{meas}} - p_O(\eta^{\text{jet}}, \mathcal{L}, p_T^{\text{jet}})}{R_{\text{jet}}(\eta^{\text{jet}}, p^{\text{jet}})} \quad (1)$$

where p_O denotes an offset correction, and R_{jet} is a correction for the response of the calorimeter to jets. A true jet is defined as being composed of only the final-state particle momenta from the hard parton-parton scatter (i.e., before interaction in the calorimeter). Although Eq. (1) is valid for any jet algorithm, p_O and the components of R_{jet} depend on the details of the jet algorithm. Our calibration procedure attempts to correct calorimeter-level jets (after interactions in the calorimeter) to their particle-level (before the individual particles interact in the calorimeter), using the described k_{\perp} jet algorithm, with $D = 1.0$. The procedure follows closely that of the calibration of the fixed-cone jet algorithm [12]. The fixed-cone jet algorithm requires an additional scale factor in Eq. (1), but we find no need for that kind of calorimeter-showering correction in the k_{\perp} jet momentum calibration [13].

The jet momentum response, $R_{\text{jet}}(\eta^{\text{jet}}, p^{\text{jet}})$, is determined as in Ref. [12], using conservation of p_T in photon-jet (γ -jet) events.

The offset p_O corresponds to the contribution to the momentum of a reconstructed jet that is not associated with the hard interaction. It contains two parts:

$$p_O = O_{\text{ue}} + O_{\text{zb}},$$

where O_{ue} is the offset due to the underlying event, and O_{zb} is an offset due to the overall detector environment. O_{zb} is attributed to any additional energy in the calorimeter cells of a jet from the combined effects of uranium noise, multiple interactions, and pile-up. The contributions of O_{ue} and O_{zb} to k_{\perp} jets are measured separately, but using similar methods. The method overlays zero-bias (random $p\bar{p}$ crossings) or min-bias (a crossing with a hard collision) $D\bar{O}$ data and Monte Carlo events, as described in Ref. [9].

The two terms of the offset correction O_{zb} and O_{ue} for k_{\perp} jets ($D = 1$) are shown in Fig. 3. Using this method for both the k_{\perp} ($D = 1$) and cone ($R = 0.7$) algorithms, the offset for the former is

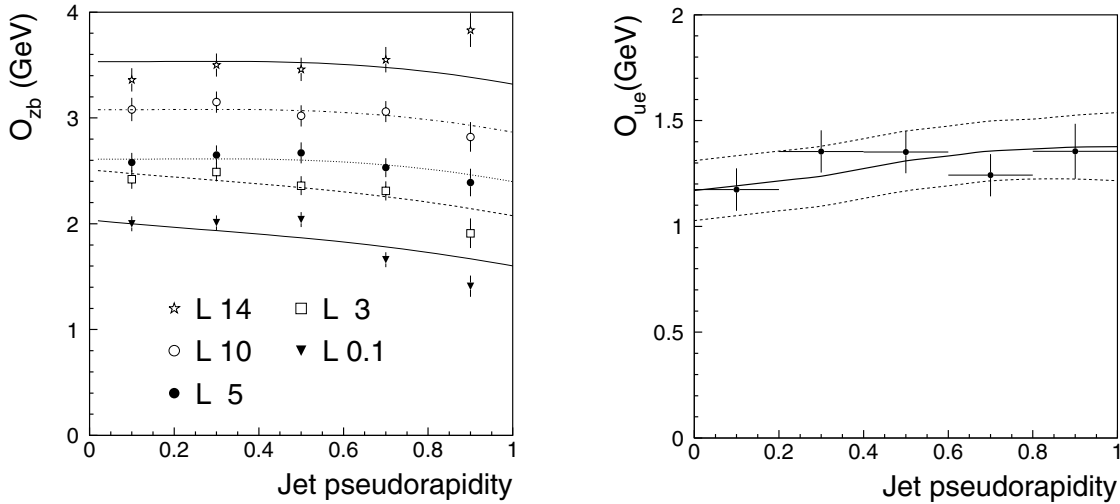


Figure 3: The offset correction terms O_{zb} and O_{ue} as a function of the pseudorapidity of the k_{\perp} jet ($D = 1.0$). The offset O_{zb} accounts for the combined effects of pile-up, uranium noise, and multiple interactions. The different sets of points are for events with different instantaneous luminosity $\mathcal{L} \approx 14, 10, 5, 3, 0.1 \times 10^{30} \text{ cm}^{-2} \text{ s}^{-1}$. The curves are fits to the points at different \mathcal{L} . The dashed curves in the O_{ue} plot denote the one standard deviation (s.d.) systematic error.

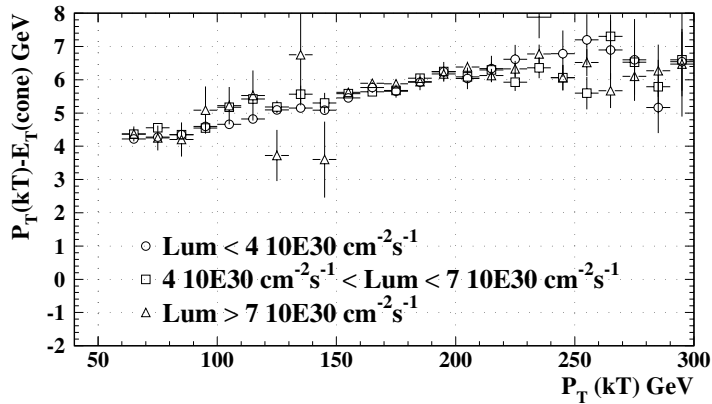


Figure 4: p_T of k_{\perp} jets ($D = 1.0$) minus E_T of the associated cone jets ($R = 0.7$) for samples taken at different instantaneous luminosities.

found to be approximately 40 – 50% larger than for the latter. In both cases, however, the offset is determined with similar absolute accuracy.

It is of interest to compare the momenta of k_{\perp} jets to those of jets reconstructed with the DØ fixed-cone algorithm [14]. For the same energy clusters the p_T of k_{\perp} jets ($D = 1.0$) is higher than the E_T of associated cone jets ($R = 0.7$). The difference increases approximately linearly with jet p_T , from about 5 GeV (or 6%) at $p_T \approx 90$ GeV to about 8 GeV (or 3%) at $p_T \approx 240$ GeV [9]. Fig. 4 shows that this difference does not depend on the instantaneous luminosity of the sample. In other words, after offset subtraction, it is clear that there is no remaining contamination in k_{\perp} jets coming from uranium noise, multiple interactions, or pile-up.

The fractional momentum resolution for k_{\perp} jets ($D = 1.0$) jets is determined from imbalance in p_T in two-jet events [15]. At 100 (400) GeV, the fractional resolution is 0.061 ± 0.006 (0.039 ± 0.003). In principle, k_{\perp} jets should be less sensitive than cone $R = 0.7$ jets to calorimeter showering fluctuations. At the same time the former is more sensitive than the latter to fluctuations in the offset. Within statistical and systematic uncertainties, however, there is not a significant difference between the measured k_{\perp} jets ($D = 1.0$) and cone $R = 0.7$ resolutions.

5. Physics Measurements

DØ has tested the k_{\perp} algorithm on Run I data by performing a number of measurements on jet production, and jet and event structure. We have studied subjet multiplicities in quark and gluon jets [9], and measured the central ($|\eta| < 0.5$) inclusive jet cross section [10]. An article on thrust distributions in jet events is in preparation.

5.1. Subjet Multiplicities

In LO QCD, the fraction of final state jets which are gluons decreases with $x \sim p_T/\sqrt{s}$, the momentum fraction of initial state partons within the proton. For fixed p_T , the gluon jet fraction decreases when \sqrt{s} is decreased from 1800 GeV to 630 GeV. We define gluon and quark enriched jet samples with identical cuts in events at $\sqrt{s} = 1800$ and 630 GeV to reduce experimental biases and systematic effects. Of the two highest p_T jets in the event, we select k_{\perp} ($D = 0.5$) jets with $55 < p_T < 100$ GeV and $|\eta| < 0.5$.

There is a simple method to extract a measurement of quark and gluon jets on a statistical basis. If M is the subjet multiplicity in a mixed sample of quark and gluon jets, it may be written as a linear combination of subjet multiplicity in gluon and quark jets:

$$M = fM_g + (1 - f)M_q \quad (2)$$

The coefficients are the fractions of gluon and quark jets in the sample, f and $(1 - f)$, respectively. Consider Eq. (2) for two similar samples of jets at $\sqrt{s} = 1800$ and 630 GeV, assuming M_g and M_q are independent of \sqrt{s} . The solutions are

$$M_q = \frac{f^{1800}M^{630} - f^{630}M^{1800}}{f^{1800} - f^{630}} \quad (3)$$

$$M_g = \frac{(1 - f^{630})M^{1800} - (1 - f^{1800})M^{630}}{f^{1800} - f^{630}} \quad (4)$$

where M^{1800} and M^{630} are the experimental measurements in the mixed jet samples at $\sqrt{s} = 1800$ and 630 GeV, and f^{1800} and f^{630} are the gluon jet fractions in the two samples. The method relies on knowledge of the two gluon jet fractions, which are extracted from the HERWIG 5.9[16] Monte Carlo event generator and used in Eqs. (3-4).

Figure 5 (left) shows the average $y_{cut} = 10^{-3}$ subjet multiplicity for quark and gluon jets. M_g is significantly larger for gluon jets than for quark jets. The gluon jet fractions are the dominant source of systematic error. We also compute the ratio $R = \frac{\langle M_g \rangle - 1}{\langle M_q \rangle - 1} = 1.84 \pm 0.15(\text{stat})_{-0.18}^{+0.22}(\text{sys})$. Figure 5 (right) shows a comparison between the ratio measured by DØ, the HERWIG 5.9 result of $r=1.91$, the ALEPH[17] value of $r=1.7 \pm 0.1$ (e^+e^- annihilations at $\sqrt{M_Z} = M_Z$), and the associated Monte Carlo and resummation prediction [18]. Good agreement is observed. All of the experimental and theoretical values for r are smaller than the naive QCD prediction of the ratio of color charges of 2.25. This is because of higher-order radiation in QCD, which tends to reduce the ratio from the naive value.

5.2. Central Inclusive Jet Cross Section

The inclusive jet cross section for $|\eta| < 0.5$, $d^2\sigma/(dp_T d\eta)$, was measured as $N/(\Delta\eta\Delta p_T\varepsilon L)$, where $\Delta\eta$ and Δp_T are the η and p_T bin sizes, N is the number of jets reconstructed with the k_{\perp} ($D = 1$) algorithm in that bin, ε is the overall efficiency for jet and event selection, and L represents the integrated luminosity of the data sample [10].

The fully corrected cross section for $|\eta| < 0.5$ is shown in Fig. 6 (left), along with the statistical uncertainties. The systematic uncertainties include contributions from jet and event selection, unsmearing, luminosity, and the uncertainty in the momentum scale, which dominates at all

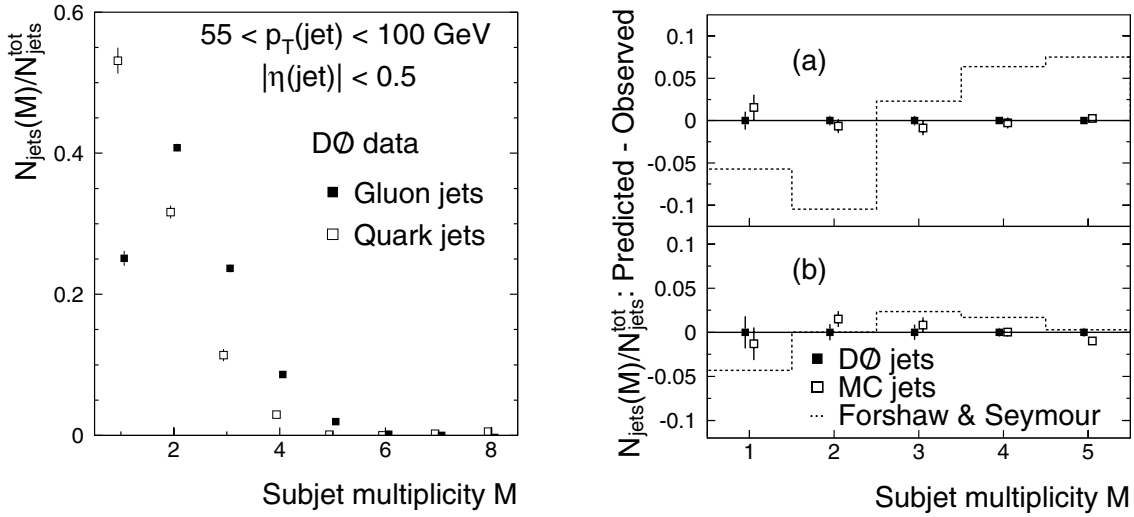


Figure 5: Left: Corrected subjet multiplicity for gluon and quark jets, extracted from DØ data. Right: the subjet multiplicity in (a) gluon and (b) quark jets, for DØ data, for the HERWIG Monte Carlo, and resummed predictions.

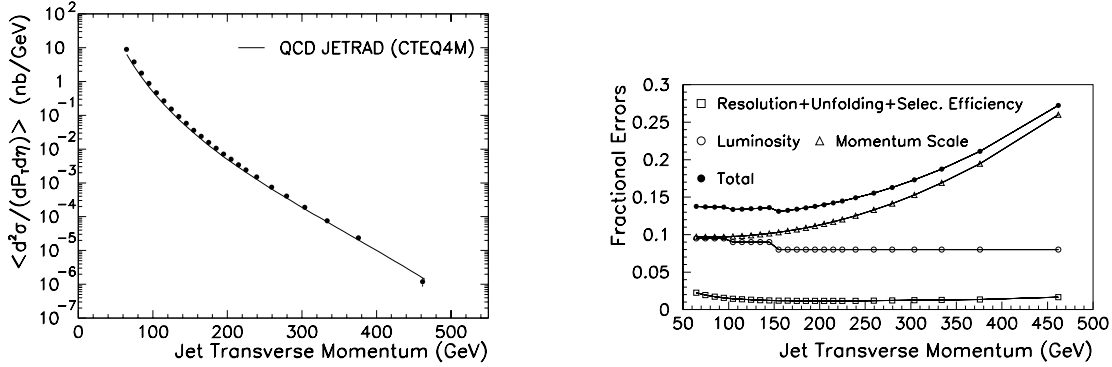


Figure 6: Left: the central ($|\eta| < 0.5$) inclusive jet cross section obtained with the k_{\perp} algorithm at $\sqrt{s} = 1.8$ TeV. Only statistical errors are included. The solid line shows a prediction from NLO pQCD. Right: fractional experimental uncertainties on the cross section.

transverse momenta. The fractional uncertainties for the different components are plotted in Fig. 6 (right) as a function of the jet transverse momentum.

The results are compared to the pQCD NLO prediction from JETRAD [19], with the renormalization and factorization scales set to $p_T^{\text{max}}/2$, where p_T^{max} refers to the p_T of the leading jet in an event. The comparisons are made using parameterizations of the parton distribution functions (PDFs) of the CTEQ [20] and MRST [21] families. Figure 7 (left) shows the ratios of (data-theory)/theory. The predictions lie below the data by about 50% at the lowest p_T and by (10–20)% for $p_T > 200$ GeV. To quantify the comparison in Fig. 7 (left), the fractional systematic uncertainties are multiplied by the predicted cross section, and a χ^2 comparison, using the full correlation matrix, is carried out [2]. Though the agreement is reasonable (χ^2/dof ranges from 1.56 to 1.12, the probabilities from 4 to 31%), the differences in normalization and shape, especially at low p_T , are quite large. The points at low p_T have the highest impact on the χ^2 . If the first four data points are not used in the χ^2 comparison, the probability increases from 29% to 77% when using the CTEQ4HJ PDF.

While the NLO predictions for the inclusive cross section for k_{\perp} ($D = 1.0$) and cone jets ($R = 0.7$, $R_{\text{sep}} = 1.3$ in the same $|\eta| < 0.5$ interval) are within 1% of each other for the p_T range of this analysis [15], the measured cross section using k_{\perp} is 37% (16%) higher than the previously reported cross section using the cone algorithm [22] at 60 (200) GeV. This difference in the cross sections is consistent with the measured difference in p_T for cone jets matched in $\eta - \phi$ space to k_{\perp} jets

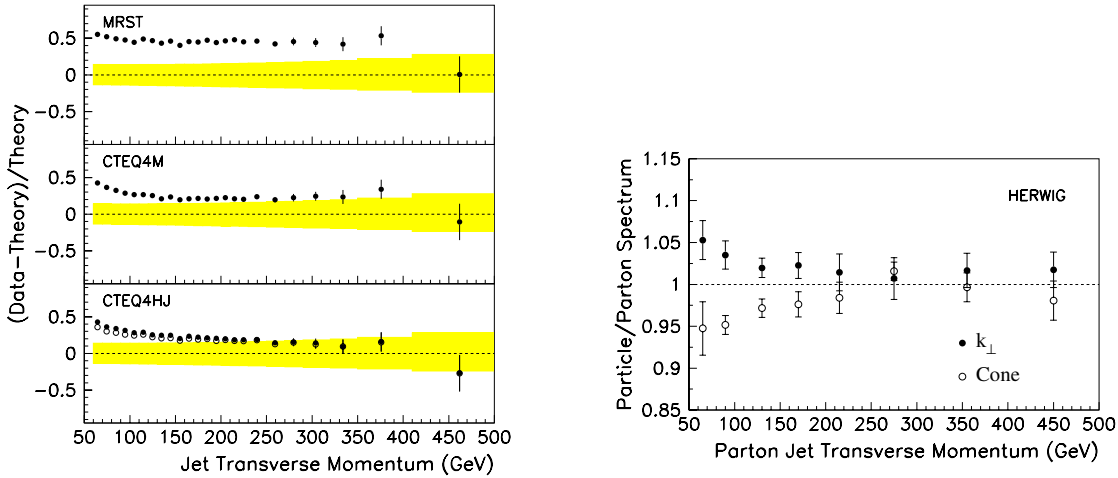


Figure 7: Left: difference between data and JETRAD pQCD, normalized to the predictions. The shaded bands represent the total systematic uncertainty. In the bottom plot a HERWIG hadronization contribution has been added to the prediction (open circles). Right: ratio of particle-level over parton-level HERWIG p_T spectra for jets, as a function of the parton jet transverse momentum.

(see Sec. 4).

The effect of final-state hadronization on reconstructed energy, which might account for the discrepancy between the observed cross section using k_\perp and the NLO predictions at low p_T , and also for the difference between the k_\perp and cone results, was studied using HERWIG (version 5.9) simulations. Figure 7(right) shows the ratio of p_T spectra for particle-level to parton-level jets, for both the k_\perp and cone algorithms. Particle cone jets, reconstructed from final state particles (after hadronization), have less p_T than the parton jets (before hadronization), because of energy loss outside the cone. In contrast, k_\perp particle jets are more energetic than their progenitors at the parton level, due to the merging of nearby partons into a single particle jet. Including the hadronization effect derived from HERWIG in the NLO JETRAD prediction improves the χ^2 probability from 29% to 44% (31% to 46%) when using the CTEQ4HJ (MRST) PDF. We have also investigated the sensitivity of the measurement to the modeling of the background from spectator partons through the use of minimum bias events, and found that it has a small effect on the cross section: at low p_T , where the sensitivity is the largest, an increase of as much as 50% in the underlying event correction decreases the cross section by less than 6%.

5.3. Event Shapes

In this section, we describe a $D0$ measurement which is in the process of being finalized: thrust distributions.

Event shape variables have been extensively used in e^+e^- and ep collider experiments to study the spatial distribution of hadronic final states, to test the predictions of perturbative QCD, and to extract a precise value of the coupling constant α_s . Over the last few years, they have attracted considerable interest, as they have proved to be a fruitful testing ground for recent QCD developments like resummation calculations and non-perturbative corrections.

There are several observables which characterize the shape of an event. To be calculable by perturbation theory, these quantities must be infra-red safe, *i.e.* insensitive to the emission of soft or collinear gluons. A widely used variable that meets this requirement is the thrust, defined as

$$T = \max_{\hat{n}} \frac{\sum_i |\vec{p}_i \cdot \hat{n}|}{\sum_i |\vec{p}_i|} \quad (5)$$

where the sum is over all partons, particles or calorimeter towers in the event. The unit vector \hat{n} that maximizes the ratio of the sums is called the thrust axis. The values of thrust range from $T = 0.5$ for a perfectly spherical event, to $T = 1$ for a pencil-like event, when all emitted particles are collinear. In this latter case, the thrust axis lies along the direction of the particles.

In most of the kinematic range, e^+e^- and ep collider experiments [23] report good agreement of event shape distributions with $O(\alpha_s^2)$ pQCD corrections to the lowest order QED diagram that governs the interaction. Fixed order QCD calculations, however, fail when two widely different energy scales are involved in the event, leading to the appearance of large logarithmic terms at all orders in the perturbative expansion [24]. This happens in the limit of the 2-jet back-to-back configuration, when $T \rightarrow 1$. This case is handled by a pQCD technique, resummation, which identifies the large logarithms in each order of perturbation theory and sums their contributions to all orders. DELPHI reports excellent agreement of thrust distributions in $Z \rightarrow$ hadrons once resummation and hadronization corrections are added to the $O(\alpha_s^2)$ QCD prediction [25].

In a hadron collider, it is convenient to introduce “transverse thrust”, T^t , a Lorentz invariant quantity under z -boosts, which is obtained from Eq. 5 in terms of transverse momenta:

$$T^t = \max_{\hat{n}} \frac{\sum_i |\vec{p}_{T_i} \cdot \hat{n}|}{\sum_i |\vec{p}_{T_i}|} \quad (6)$$

Transverse thrust ranges from $T^t = 1$ to $T^t = 2/\pi$ ($\langle |\cos \theta| \rangle$) for a back-to-back and an isotropic distribution of particles in the transverse plane, respectively. To minimize systematics associated with the busy environment of a $p\bar{p}$ collider, we use only the two leading jets in the event, reconstructed with a $k_\perp D = 1$ algorithm, rather than using all calorimeter towers. Other particles in the event are inferred from the angular distribution of the two leading jets.

The observable proposed by DØ is, therefore, the Dijet Transverse Thrust, binned in terms of $H_{T3} = p_{T1} + p_{T2} + p_{T3}$. H_{T3} , defined as the scalar sum of the transverse momenta of the three leading jets of the event, is an estimator of the energy scale of the event. The lowest order at which pQCD does not give the trivial result $T = 1$ is $O(\alpha_s^3)$, corresponding to up to three parton jets in the final state. A $O(\alpha_s^3)$ calculation, like JETRAD, does not cover the whole physical range of T_2^t . In the interval $\sqrt{2}/2 < T_2^t < \sqrt{3}/2$, the LO perturbative contribution is of order $O(\alpha_s^4)$. A $O(\alpha_s^3)$ prediction will also fail at $T \rightarrow 1$, where events with two back-to-back jets plus soft radiation contribute large logarithms which need to be resummed.

The measurement proposed in this section presents a good opportunity to test resummation models, as well as the recently developed NLO pQCD three-jet generators [26].

6. Summary and Perspectives for Run II

DØ has implemented and studied a k_\perp jet algorithm for the first time in a hadron collider. The $D = 1$ k_\perp algorithm is more sensitive than the cone $R = 0.7$ algorithm to spurious energy depositions from the underlying event, noise, pile-up, and multiple interactions. This effect, however, can be removed from both algorithms with the same degree of accuracy. Moreover, the $D = 1$ k_\perp algorithm is less sensitive than the cone $R = 0.7$ algorithm to calorimeter showering effects. Differences in energy resolutions for both algorithms are not significant.

We have submitted two results for publication: the subjet multiplicity in quark and gluon jets and the central inclusive jet cross section measurements. A third one, a measurement of the event thrust distributions, is underway. The DØ subjet multiplicity result demonstrates that gluon and quark jets are significantly different in hadron collisions, and that it may be possible to discriminate between them on an individual basis. The DØ $D = 1$ k_\perp inclusive jet cross section is in reasonable agreement with NLO pQCD predictions, except at low p_T where the agreement is marginal. The agreement improves by incorporating a hadronization correction. Thrust distribution measurements will be a useful tool to study the significance of resummation calculations, as well as the recently developed NLO pQCD three-jet generators.

In Run II, the larger data sample and the higher center-of-mass energy will allow DØ to extend the energy reach of previous measurements, as well as to search for quark compositeness at a higher energy scale. The low p_T region ($p_T < 50$ GeV), as well as the underlying event, will hopefully be explored with more accuracy with the aid of the upgraded tracking system. With the addition of a central magnetic field, energy scale and resolution uncertainties will be reduced. A combination of measurements using several algorithms and samples taken at different center-of-mass energies is desirable to understand and distinguish with higher accuracy between instrumentation and physics effects.

References

- [1] J. Huth *et al.*, in *Proc. of Research Directions for the Decade, Snowmass 1990*, edited by E.L. Berger (World Scientific, Singapore, 1992).
- [2] B. Abbott *et al.* (DØ Collaboration), *Phys. Rev. D* **64** 032003 (2001).
- [3] T. Affolder *et al.* (CDF Collaboration), *Phys. Rev. D* **64** 032001 (2001).
- [4] S.D. Ellis, Z. Kunszt and D.E. Soper, *Phys. Rev. Lett.* **69** , 3615 (1992).
- [5] W.T. Giele and W.B. Kilgore, *Phys. Rev. D* **55** 7183 (1997).
- [6] S. Catani, Yu.L. Dokshitzer, M.H. Seymour, and B.R. Webber, *Nucl. Phys.* **B406** 187 (1993).
- [7] S. Catani, Yu.L. Dokshitzer, and B.R. Webber, *Phys. Lett. B* **285** 291 (1992).
- [8] S.D. Ellis and D.E. Soper, *Phys. Rev. D* **48** 3160 (1993).
- [9] V.M. Abazov *et al.* (DØ Collaboration). Submitted to *Phys. Rev. D.*, hep-ex/0108054.
- [10] V.M. Abazov *et al.* (DØ Collaboration). Submitted to *Phys. Rev. Lett.*, hep-ex/0109041.
- [11] S. Abachi *et al.* (DØ Collaboration), *Nucl. Instrum. Methods in Phys. Res. A* **338**, 185 (1994).
- [12] B. Abbott *et al.* (DØ Collaboration), *Nucl. Instrum. Meth. A* **424**, 352 (1999).
- [13] K.C. Frame (for the DØ Collaboration), in *Proceedings of the VIII International Conference on Calorimetry in High Energy Physics*, edited by G. Barreira, B. Tome, A. Gomes, A. Maio, and M. J. Varanda
- [14] W. Giele *et al.* (Jet Physics Working Group), in *QCD and Weak Boson Physics in Run II*, edited by U. Baur, R.K. Ellis, D. Zeppenfeld (Fermilab, Batavia, IL, 2000).
- [15] S. Grinstein, Ph.D. thesis, Univ. de Buenos Aires, Argentina, 2001 (in preparation).
- [16] G. Marchesini, B.R. Webber, G. Abbiendi, I.G. Knowles, M.H. Seymour, and L. Stanco, *Comp. Phys. Comm.* **67**, 465 (1992).
- [17] D. Buskulic *et al.* (ALEPH Collaboration), *Phys. Lett. B* **346**, 389 (1995).
- [18] M.H. Seymour, *Phys. Lett. B* **378**, 279 (1996).
- [19] W.T. Giele, E.W.N. Glover, and D.A. Kosower, *Phys. Rev. Lett.* **73** , 2019 (1994).
- [20] H.L. Lai *et al.*, *Phys. Rev. D* **55**, 1280 (1997).
- [21] A. D. Martin *et al.*, *Eur. Phys. J. C* **4**, 463 (1998).
- [22] B. Abbott *et al.* (DØ Collaboration), *Phys. Rev. Lett.* **86** 1707 (2001).
- [23] ALEPH Collaboration, D. Decamp *et al.*, *Phys. Lett* **B234** 399 (1990); *Phys. Lett* **B255** 623 (1991). DELPHI Collaboration, P. Aarnio *et al.*, *Phys. Lett.* **B240** 271 (1990). L3 Collaboration, B. Adeva *et al.*, *Phys. Lett.* **B237** 136 (1990) OPAL Collaboration, M.Z. Akrawy *et al.*, *Phys. Lett.* **B235** 389 (1990); *Z. Phys.* **C47** 505 (1990) 505. TASSO Collaboration, W. Bartel *et al.*, *Z.Phys.* **C33** 187 (1990).
- [24] OPAL Collaboration, K. Ackerstaff *et al.*, *Z.Phys.* **C75** 193 (19 97). DELPHI Collaboration, P. Abreu *et al.*, *Z.Phys.* **C73** 229 (1997). H1 Collaboration, C. Adloff *et al.*, *Phys.Lett.* **B406** 256 (1997). K. Rabbertz and U. Wollmer hep-ex/0008006; G. J. McCance hep-ex/0008009; G.P.Korchemsky and S.Tafat hep-ph/0007005; Y. Dokshitzer hep-ph/9911299; O. Biebel, P. Movilla and S. bethke, *Phys.Lett.* **B459** 326 (1999); S. Catani, L. Trentadue, G. turnock and B. Webber *Phys.Lett.* **B263** 491 (1991); G.P.Korchemsky and G.Sterman, *Nucl.Phys.* **B555** 335 (1999).
- [25] M. Seymour, *Nucl. Phys.* **B513** 269 (1998); J. Forshaw and M.H. Seymour, *JHEP* 09 009(1999); W. Giele, E. Glover and D. Kosower, hep-ph/9706210.
- [26] W. Kilgore, W. Giele, ICHEP 2000, Osaka, Japan (hep-ph/0009193).